

# Genome-wide analysis of genetic pleiotropy and causal genes across three age-related ocular disorders

Xueming Yao,<sup>1</sup> Hongxi Yang,<sup>2,a</sup> Han Han,<sup>1</sup> Xuejing Kou,<sup>1</sup> Yuhang Jiang,<sup>3</sup> Menghan Luo,<sup>3</sup> Yao Zhou,<sup>3</sup> Jianhua Wang,<sup>3</sup> Xutong Fan,<sup>3</sup> Xiaohong Wang,<sup>2,\*</sup> Mulin Jun Li,<sup>2,3,\*</sup> Hua Yan<sup>1,\*</sup>

<sup>1</sup> Department of Ophthalmology, Tianjin Medical University General Hospital, Tianjin, 300052, China.

<sup>2</sup> Department of Pharmacology, Tianjin Key Laboratory of Inflammation Biology, School of Basic Medical Sciences, Tianjin Medical University, Tianjin, 300070, China.

<sup>3</sup> Department of Bioinformatics, The Province and Ministry Co-sponsored Collaborative Innovation Center for Medical Epigenetics, School of Basic Medical Sciences, Tianjin Medical University, Tianjin, 300070, China.

\*Correspondence: [xiaohongwang@tmu.edu.cn](mailto:xiaohongwang@tmu.edu.cn) (X.W.), [mulin@tmu.edu.cn](mailto:mulin@tmu.edu.cn) (M.J.L.), [zyyanyanhua@tmu.edu.cn](mailto:zyyanyanhua@tmu.edu.cn) (H.Y.)

---

<sup>a</sup> X.Y. and H.Y. contributed equally.

## 17    **Abstract**

18    Age-related macular disorder (AMD), cataract, and glaucoma are leading causes of blindness  
19    worldwide. Previous genome-wide association studies (GWASs) have revealed a variety of  
20    susceptible loci associated with age-related ocular disorders, yet the genetic pleiotropy and causal  
21    genes among these diseases remain poorly understood. By leveraging large-scale genetic and  
22    observational data from ocular disease GWASs and UK Biobank (UKBB), we found significant  
23    pairwise genetic correlations and epidemiological associations for these ocular disorders.  
24    Cross-disease meta-analysis uncovered ten pleiotropic loci, four of which were replicated in an  
25    additional cohort. Integration of variants in pleiotropic loci and multiple single-cell omics data  
26    identified that Müller cells and astrocytes were likely causal cell types underlying ocular  
27    comorbidity. In addition, we comprehensively integrated eye-specific gene expression quantitative  
28    loci (eQTLs), epigenomic profiling, and 3D genome data to prioritize causal pleiotropic genes. We  
29    found that pleiotropic genes were essential in nerve development and eye pigmentation, and  
30    targetable by existing drugs for the treatment of single ocular disorder. These findings will not  
31    only facilitate the mechanistic research of ocular comorbidities but also benefit the therapeutic  
32    optimization of age-related ocular diseases.

33

## 34 Introduction

35 Age-related ocular diseases, such as age-related macular degeneration (AMD), cataract, and  
 36 glaucoma, are among the leading causes of irreversible blindness and vision impairment in adults  
 37 aged  $\geq 50$  years worldwide <sup>1</sup>. Previous cross-sectional and case-control studies have reported that  
 38 cataract and glaucoma commonly co-exist and prevalent glaucoma is associated with neovascular  
 39 AMD <sup>2;3</sup>. A clinical study also showed that over 20% of eye samples from the patients listed for  
 40 cataract surgery have evidence of AMD according to optical coherence tomography imaging <sup>4</sup>.  
 41 The findings motivate the exploration of the extent and causal factors for potential comorbidity  
 42 among these age-related ocular diseases.

43  
 44 Recent genome-wide association studies (GWASs) have identified hundreds of genetic signals that  
 45 contribute to the complex pathogenesis of AMD <sup>5;6</sup>, cataract, <sup>7</sup> and glaucoma <sup>8-10</sup>. These and other  
 46 genetic studies also suggest a high heritability in susceptibility of AMD (~50%) <sup>11</sup>, cataract  
 47 (35-58%) <sup>12;13</sup>, and glaucoma (35-65%) <sup>14;15</sup>. Nevertheless, the shared genetic architecture among  
 48 these age-related ocular diseases is largely unknown. A study investigated the genetic pleiotropy  
 49 among AMD and several eye-related diseases/traits, and found that patients with AMD  
 50 demonstrate a genetically reduced risk to develop open-angle glaucoma <sup>16</sup>, which is inconsistent  
 51 with other findings <sup>17;18</sup>. Moreover, no genetic pleiotropy research has been conducted between  
 52 cataract and other ocular diseases so far. Given the conflicting results and scant knowledge  
 53 regarding the shared genetic architecture of these age-related ocular disorders, more systematic  
 54 investigation based on larger and complementary cohorts is needed.

55

56 While different levels of genetic correlations or pleiotropic loci can be faithfully estimated among  
57 ocular diseases/traits, the pleiotropic genes and causal variants have not been rigorously examined.  
58 This is an important issue to clarify, as the shared biological basis of ocular disorders could  
59 represent potential efficient intervention targets for the prevention and treatment of ocular  
60 comorbidities. Emerging tissue/cell type-specific epigenomic profiles, single-cell omics atlas as  
61 well as molecular phenotype quantitative trait loci (QTLs) mapping on certain ocular diseases  
62 revealed many causal variants and genes underlying cell type specificity of disease etiology<sup>19-23</sup>.  
63 Thus, integrating large-scale multi-omics and QTL data from eyes with disease pleiotropy  
64 information would provide a promising strategy to decipher the genetic causality of ocular  
65 comorbidities, especially for the majority of causal variants in the non-coding genomic regions.

66  
67 Here, by leveraging large-scale genetic and observational data from public GWASs and UK  
68 Biobank (UKBB), we systematically investigated the genetic sharing patterns and epidemiological  
69 associations of three age-related ocular diseases including AMD, cataract, and glaucoma. We  
70 found extensive genetic pleiotropy and pairwise connections among these three diseases and  
71 identified ten pleiotropic loci across the genome. To better understand the mechanism underlying  
72 these pleiotropic loci, the integration of eye-specific gene expression (eQTLs), epigenomic  
73 profiling, and 3D genome data were conducted to probe causal pleiotropic genes. Finally, drug  
74 repurposing was conducted by utilizing molecular networks for potential treatment or prevention  
75 of ocular comorbidities.

76

## 77 **Material and methods**

## 78 **GWAS summary statistics collection**

79 Full GWAS summary statistics of European ancestry on AMD, cataract, and glaucoma with the  
80 largest sample size were obtained after searching eight databases (GWAS Catalog <sup>24</sup>, UKBB <sup>25</sup>,  
81 GeneAtlas <sup>26</sup>, GWAS Atlas <sup>27</sup>, LD Hub <sup>28</sup>, GRASP <sup>29</sup>, PhenoScanner <sup>30</sup>, and dbGaP <sup>31</sup>). GWAS  
82 summary statistics with available signed statistics (beta or odds ratio), effect alleles, and  
83 non-effect alleles were retained during the search. We also collected GWAS summary data from  
84 FinnGen for replication analysis <sup>32</sup>. More detailed information regarding the selected GWAS  
85 summary statistics for AMD, cataract, and glaucoma was shown in **Table S1**.

86

## 87 **Estimation of genetic correlation**

88 Using GWAS summary statistics derived from the above datasets with a sample size > 50,000 and  
89 the number of cases and controls > 10,000, we conducted LD Score regression (LDSC) <sup>33</sup> for  
90 these ocular diseases to estimate pairwise genetic correlations. SNPs were filtered to HapMap3  
91 SNPs to avoid bias due to inconsistent imputation quality. SNPs with INFO  $\leq 0.9$ , minor allele  
92 frequency  $\leq 0.01$ , non-SNP variants, strand-ambiguous SNPs, and SNPs with duplicate IDs were  
93 removed. Pre-computed linkage disequilibrium (LD) scores and regression weights for European  
94 populations of the 1000 Genomes project were downloaded from the LDSC website  
95 ([http://www.broadinstitute.org/~bulik/eur\\_ldscores/](http://www.broadinstitute.org/~bulik/eur_ldscores/)). We ensured that the LD score regression  
96 intercepts for AMD, cataract, and glaucoma were close to 1 during estimations. Moreover, genetic  
97 correlations between these diseases were also estimated using another tool SumHer from LDAK <sup>34</sup>  
98 under the recommended LDAK-Thin model. A tagging file computed using 2,000 white British  
99 individual genetic data files was downloaded from the LDAK website

(<https://dougsspeed.com/pre-computed-tagging-files/>), and the cutoff was set to 0.01 to preclude large-effect loci that explain at least 1% of phenotypic variance.

102

### 103 **Mendelian randomization**

104 Mendelian randomization (MR) analysis between two traits was performed to determine whether  
105 genetic correlations were due to a causal link or confounding factors using the R package  
106 TwoSampleMR<sup>35</sup> which encompasses five MR methods (MR Egger, Weighted median, Inverse  
107 variance weighted, Simple mode, Weighted mode). The instruments for each exposure trait were  
108 significant SNPs ( $P\text{-value} < 5 \times 10^{-8}$ ) after clumping, while the instruments for each outcome  
109 trait were all SNPs. Variants without SNP ID were annotated using the dbSNP<sup>36</sup> database;  
110 otherwise, SNPs were removed during subsequent analyses.

111

### 112 **Epidemiological analyses based on UK Biobank (UKBB) cohort**

113 The UKBB is a large-scale cohort that recruited half a million UK participants (aged 37–73 years)  
114 between 2006 and 2010, and was followed up to 2021. Among the 502,412 participants, we  
115 excluded those who were pregnant ( $n = 379$ ), lost to follow-up ( $n = 1,298$ ), and had a mismatch  
116 between self-reported sex and genetic sex ( $n = 371$ ), or missing information concerning covariates  
117 at baseline ( $n = 58,637$ ). Overall, 441,727 participants were included in the study. AMD (ICD10:  
118 H35.3; ICD9: 362.5), cataract (ICD10: H25-H28; ICD9: 366), and glaucoma (ICD10: H40.1,  
119 H40.8, H40.9; ICD9: 365.1, 365.9) were ascertained based on information from self-reports,  
120 primary care records, hospital admissions, and death records. Multivariate Cox regression with  
121 separate models for incident AMD, cataract, and glaucoma was used to evaluate pairwise

122 associations among them. In subsequent analyses, multi-state models were used to examine the  
123 role of one of the three ocular diseases in the transition between the start of follow-up and the  
124 other two disorders. In all models, we adjusted for sex, age, ethnicity, Townsend deprivation index,  
125 education level, smoking status, drinking status, physical activity, screen time-based sedentary  
126 behavior, diabetes, and other eye problems. This research was conducted using the UKBB  
127 resource under application number 83974.

128

### 129 **Determination of pleiotropic regions**

130 We performed pleiotropic region analysis using gwas-pw<sup>37</sup>, a tool for jointly analyzing pairs of  
131 GWAS traits. Overlapping SNPs of both traits were split into multiple blocks based on the bed  
132 files available at <https://bitbucket.org/nygcresearch/ldetect-data>. Separately, gwas-pw reckoned the  
133 posterior probability of the four models that the pleiotropic region 1) only associated with  
134 phenotype 1, 2) only associated with phenotype 2, 3) associated with both phenotypes, and 4)  
135 associated with both phenotypes independently.

136

### 137 **Identification of pleiotropic loci**

138 To identify pleiotropic variants and characterize pleiotropy at single-variant level, cross-trait  
139 meta-analyses were carried out with GWAS summary statistics of three ocular diseases using three  
140 different approaches: 1) ASSET<sup>38</sup>, 2) METAL<sup>39</sup>, and 3) pleioFDR<sup>40</sup>. ASSET explored all  
141 possible subsets of traits and evaluated a fixed-effect meta-analysis for each subset. The default  
142 scheme was selected when executing METAL with the correction of sample overlap. pleioFDR  
143 leveraged overlapping SNP associations of related phenotypes to identify genetic pleiotropic loci.

144 All significant SNPs involving two or more traits were retained for the following analysis. Once  
145 classified, we conducted variant clumping through PLINK <sup>41</sup> and merged the pleiotropic loci if  
146 they physically overlapped ( $\pm 250\text{kb}$ ). The summary statistics of these diseases were standardized  
147 using a downloaded reference derived from genome files for 22 autosomes of filtered the 1000  
148 Genomes project <sup>42</sup> European ancestry samples.

149

# **150 Causal cell type estimation**

151 We applied MAGMA <sup>43</sup> to evaluate whether specific ocular cell types showed significant  
152 heritability enrichment for traits based on ASSET one-sided summary statistics. MAGMA also  
153 requires gene average expression level across cell types derived from single-cell RNA sequencing  
154 (scRNA-seq) and single-cell multi-omics sequencing data of anterior chamber angle or  
155 retina/choroid <sup>20; 21; 23; 44-46</sup> (Table S2). We additionally downloaded the raw data and determined  
156 the average expression values per cell type for each dataset using Cell Ranger <sup>47</sup> and the R  
157 package Seurat <sup>48</sup> unless the information was available. Cell types were assigned with the gene  
158 marker mentioned in the original publications, and the same cell types were manually renamed to  
159 maintain concordance with different scRNA-seq data. Gene names were transferred to Entrez gene  
160 IDs using the R package biomaRt <sup>49</sup>. We appointed the direction of testing to “greater” and  
161 selected the condition-hide modifier for cell-type trait association analysis. We then leveraged the  
162 open chromatin peaks of retinal cell types from single-cell multiome to estimate LD scores for  
163 LDSC and conducted an additional cell-type trait association analysis.

164

# **165 Causal SNP identification at pleiotropic loci**

Colocalization analysis between two-eye eQTL data<sup>19;50</sup> and ASSET one-sided GWAS data was conducted using the R package COLOC<sup>51</sup>. We selected SNPs with an H4 posterior probability > 0.75, GWAS P-value <  $1 \times 10^{-6}$ , and eQTL P-value < 0.05 as pleiotropic loci. By utilizing three sets of retina sample Assay of Transposase Accessible Chromatin sequencing (ATAC-seq) and H3K27ac Chromatin immunoprecipitation followed by sequencing (ChIP-seq) data<sup>52</sup>, genomic enhancer regions of the retina were predicted using the Activity-by-Contact (ABC) model<sup>53</sup> with default threshold settings. Next, we profiled the causal SNPs through fine-mapping analysis of pleiotropic loci identified by the above three meta-analysis methods. The one-sided ASSET meta-analysis results of pleiotropic SNPs located in the  $\pm 1$  Mb region of lead SNPs were imported into PolyFun<sup>54</sup> for fine-mapping with an embedded statistical method termed Susie<sup>55</sup>, and 95% credible sets were revealed, assuming one causal SNP per locus. SNPs were included in the credible sets until the sum of the posterior probabilities was > 0.95.

178

### 179 **Pleiotropic causal gene prioritization**

The causal genes in a pleiotropic locus were confined to the following rules: 1) Does the locus contain eye eQTL SNPs? If yes, eQTL harboring genes (eGenes) were selected. 2) Is the locus located in the open chromatin peaks from retina H3K27ac HiChIP data<sup>23</sup>? If yes, causal genes were anchor-targeted genes. 3) Does the locus have a genomic region overlapping with the ABC model enhancer regions or a cell type-specific peak? If so, the causal genes were enhancer target genes or peak-inclusive genes. 4) If the pleiotropic locus contained none of the eQTL SNPs or was not mapped within any enhancer regions or peaks, the nearest gene with the highest COLOC posterior probability was identified as a causal gene. Moreover, gene ontology (GO) pathway

188 enrichment analysis of causal genes with no more than 10 interactors was conducted in STRING  
189 <sup>56</sup> to shed light on pathogenic biological processes, and gene-phenotype association analysis was  
190 conducted using Enrichr <sup>57</sup>.

191

## 192 **Drug repurposing analysis**

193 We curated approved drugs targeted at pleiotropic causal genes and target genes of such drugs for  
194 AMD, cataract, and glaucoma from Drugbank <sup>58</sup> and DGIdb <sup>59</sup> to verify whether the risk genes  
195 were identical to the drug target genes. Protein-protein interaction (PPI) network information was  
196 obtained from STRING and depicted using Cytoscape <sup>60</sup> to evaluate potential relationships  
197 between pleiotropic causal genes and drug target genes.

198

## 199 **Results**

### 200 **Genetic sharing among AMD, cataract, and glaucoma**

201 To delineate the shared genetic architecture among the three age-related ocular disorders, we first  
202 collected full GWAS summary statistics of AMD, cataract, and glaucoma from the latest public  
203 resources, incorporating three AMD GWASs, three cataract GWASs and two glaucoma GWASs,  
204 and most of them had sample size over 100,000 individuals (**Table S1**). Considering the signal  
205 overlaps of the three largest ocular GWAS summary statistics (**Figure S1A**), genetic correlations  
206 were measured using LDSC <sup>33</sup> and SumHer LDAK-Thin <sup>34</sup> models. Following careful quality  
207 control, we observed moderate and concordant genome-wide genetic correlations among these  
208 traits (**Figure 1A, 1B, Figure S1B**), in which glaucoma-cataract and AMD-cataract showed  
209 positive genetic correlations, while AMD-glaucoma exhibited negative genetic correlations. This

is consistent with a previous study wherein the negative genetic correlation between AMD and glaucoma was reported<sup>16</sup>. In addition, multiple bidirectional MR methods were applied to each pair of diseases to assess whether shared genetic components were coherent with true pleiotropy or mediated pleiotropy. Presuming that consistent results in three of the five MR methods indicate a strong causal effect between the two traits, there was no or weak evidence for potentially causal relationships among AMD, cataract, and glaucoma (**Figure S2**).

216

### 217 **Epidemiological associations among AMD, cataract, and glaucoma**

To test whether the pattern of genetic sharing for the three age-related ocular disorders is supported by epidemiological associations, we leveraged 441,727 selected participants from the UKBB with rich information regarding self-reports, primary care records, hospital admissions, and death records. In the UKBB cohort, at the end of follow-up, 36,5471 (82.74%) participants had no AMD, cataract, or glaucoma; 5,611 (1.27 %) had AMD alone; 48,639 (11.01%) had cataract alone; 7,431 (1.68%) had glaucoma alone; 8,251 (1.87%) had both AMD and cataract; 1,329 (0.30%) had both AMD and glaucoma; 7,015 (1.59%) had both cataract and glaucoma; and 1,010 (0.23%) had AMD, cataract, and glaucoma. Hazard ratios (HRs) estimated by Cox regression were significantly larger than 1 (P-value < 0.001), which indicated positive correlations among these traits (**Figure 1A, Figure S3**). These results showed significant pairwise associations between AMD, cataract, and glaucoma. Similar results were observed in further analyses using multi-state models which also uncovered positive correlations between cataract and other diseases as genetic correlation analysis showed. The correlation between AMD and glaucoma was inconsistent with our genetic correlation results which may due to environmental effects or inadequate power.

232 Additionally, multi-state models distinguished the roles of one of the three prevalent ocular  
233 diseases in the temporal trajectories of the other two. Prevalent glaucoma was inversely associated  
234 with AMD after cataract with HR of 0.74 (95% CI: 0.64-0.86), but not with cataract after AMD  
235 (**Figure 1C**). Multi-state analyses also showed that the associations of prevalent cataracts with the  
236 transition from the start of follow-up to subsequent AMD or subsequent glaucoma were stronger  
237 than those with the transition from AMD to glaucoma or from glaucoma to AMD (**Figure 1D**).  
238 Accounting for prevalent AMD in transitions of cataract and glaucoma, there was no evidence of  
239 stronger associations between prevalent AMD and transitions to cataract after having had  
240 glaucoma, or glaucoma after having had cataract (**Figure 1E**). Taken together, these new findings  
241 based on genetic evidence and epidemiological associations suggested a latent correlation among  
242 age-related ocular traits.

243

#### 244 **Cross-disorder meta-analysis reveals ten pleiotropic loci**

245 Considering the indication for genetic relationships between AMD-cataract, AMD-glaucoma, and  
246 cataract-glaucoma, 11 likely pleiotropic regions (posterior probability associated with two  
247 phenotypes  $> 0.6$ ) were identified in the disease pairs using gwas-pw<sup>37</sup>, one of which  
248 (chr9:20464018-2220526) turned out to be significant of two disease pairs (**Figure 1F, Table S3**).  
249 Next, we leveraged the largest collected GWAS summary statistics for AMD, cataract, and  
250 glaucoma containing 257,718 cases and 560,421 controls of European ancestry in total (AMD:  
251 14,034 cases and 91,214 controls, cataract: 11,306 cases and 349,888 controls, glaucoma: 232,378  
252 cases and 119,319 controls), and conducted cross-trait meta-analyses using three complementary  
253 methods including ASSET<sup>38</sup>, METAL<sup>39</sup> and pleioFDR<sup>40</sup>. Only those SNPs that surpassed

254 genome-wide significance ( $P\text{-value} < 5 \times 10^{-8}$ ) and had influences on at least two traits were  
 255 reserved. For ASSET, two patterns were supported, and both were performed such that the  
 256 one-sided ASSET meta-analysis maximized the standard fixed-effect meta-analysis test statistics  
 257 over all possible subsets and guaranteed the identification of pleiotropic loci that have associations  
 258 in the same direction, while the two-sided ASSET meta-analysis was performed in two directions  
 259 automatically. Accordingly, we identified 5, 10, 15, and 7 pleiotropic loci using METAL,  
 260 one-sided ASSET, two-sided ASSET, and pleioFDR, respectively, under the condition that the  
 261 genomic inflation factor did not considerably deviate from one (**Figure 2A, Figure S4, Figure**  
 262 **S5**).

263  
 264 By guaranteeing that the lead SNPs were slightly significant in all primary GWAS summary  
 265 statistics, ten loci were conservatively prioritized as candidate pleiotropic loci for which the  
 266 one-sided ASSET results overlapped with the other three approaches (**Table 1**). Among these  
 267 pleiotropic loci, most signals were significantly associated with glaucoma, and were even stronger  
 268 after meta-analysis although they were weaker in other diseases. Notably, four novel loci (lead  
 269 SNPs: rs3766916, rs17421627, rs11018564, rs146447071) became significant as the sample size  
 270 increased. Besides, we found that four candidate pleiotropic loci intersected the aforementioned  
 271 pleiotropic regions identified by gwas-pw (chr5:87390784-88891173, chr9:20464018-2220526,  
 272 chr11:87430571-89208854, chr15:110336875-113261782) (**Table 1, Figure 1F**), which rendered  
 273 our results convincing. Furthermore, we collected additional GWAS datasets of AMD, cataract,  
 274 and glaucoma from FinnGen project<sup>32</sup> and conducted a meta-analysis with ASSET, four loci (lead  
 275 SNPs: rs12670840, rs944801, rs1619882, and rs1129038) were replicated if the P-value of any

276 SNPs in the same loci was smaller than  $1 \times 10^{-5}$  in one-sided ASSET or two-sided ASSET  
277 results.

278

## 279 **Single-cell multi-omics data integration identifies likely causal cell types of ocular** 280 **comorbidity**

281 To understand the causal disease mechanisms underlying these pleiotropic loci, we investigated  
282 which cell types are essential during the development of ocular comorbidity. We obtained six  
283 scRNA-seq datasets and a single-cell multiome dataset derived from 33 human eyes (**Table S2**)  
284 and performed cell-type trait association analysis to explore the most likely causal cell types  
285 whose gene or epigenomic signatures correlate with genetic pleiotropy. In total, more than 40 cell  
286 types across the anterior chamber angle and retina/choroid were used in our study. Consequently,  
287 Müller cells and astrocytes were concordantly estimated to be two causal cell types of ocular  
288 disease susceptibility using both MAGMA and LDSC (**Figure 2B, Figure S6, Table S4, Table**  
289 **S5**), suggesting that the two cell types could play a critical role in modulating ocular comorbidity.  
290 In addition, vascular endothelium and fibroblasts also displayed significant results in two or more  
291 MAGMA analyses ( $FDR < 0.05$ ), which is consistent with previous study<sup>20</sup>.

292

## 293 **Functional prioritization of causal pleiotropic variants and their target genes**

294 To identify the causal genes acting on genetic pleiotropy across the three age-related ocular  
295 disorders,  
296 we first leveraged PolyFun<sup>54</sup> to fine-map the ten pleiotropic loci and identified causal variants in  
297 the 95% credible sets. We conducted colocalization analysis involving the ten pleiotropic loci

298 based on two retinal *cis*-eQTL datasets<sup>19;50</sup>, yielding a credible variant rs3766916 colocalizing at  
 299 several eGenes, including *TRIM46* and *GON4L* (**Figure 2C, Figure S7, Table S6**). *TRIM46*  
 300 encodes a protein of the tripartite motif family that controls neuronal polarity and  
 301 high-glucose-induced ferroptosis in human retinal capillary endothelial cells<sup>61</sup>, which suggests a  
 302 potential causal role for retina-associated ocular traits.

303

304 Second, we collected retina H3K27ac HiChIP loops<sup>23</sup> to annotate all credible variants with  
 305 spatially proximal genes. We found that three credible variants supported by HiChIP loops linked  
 306 to different genes, and they were located in the eye enhancer regions or Müller cell/astrocyte open  
 307 chromatin peaks according to single-cell multiome profiles. Notably, we found the SNP rs4845712  
 308 in high LD with rs3766916 ( $r^2 = 0.95$  in European) may be more likely to be the causal SNP at the  
 309 corresponding pleiotropic locus. rs4845712 in the intron of *EFNA4* gene received the highest  
 310 posterior probability of fine-mapping analysis and overlapped with a retina H3K27ac HiChIP loop  
 311 (**Figure 2D**). rs4845712 host gene *EFNA4* has been reported to inhibit axonal regeneration and  
 312 regulate axon guidance in the optic nerve<sup>62; 63</sup>, and its HiChIP target gene *CKS1B* encodes a  
 313 protein that binds to the catalytic subunit of cyclin-dependent kinases, and proliferation and  
 314 migration of retinoblastoma cells can be inhibited by suppressing the expression of *CKS1B*<sup>64</sup>.  
 315 Another top credible SNP rs351973, close to *PTBP1* promoter region, can interact with the  
 316 genomic region containing *KISS1R*, *R3HDM4*, and *ARID3A* genes (**Figure 3A**). Among these  
 317 genes, knockdown of *Ptbp1* in mice effectively induces the conversion of Müller glia into retinal  
 318 ganglion cells (RGCs), resulting in alleviation of disease symptoms pertinent to RGC loss<sup>65</sup>.

319

320 Additionally, we applied ABC model<sup>53</sup> on ATAC-seq and H3K27ac ChIP-seq data from three  
321 retinal samples to predict enhancer-promoter interactions (**Table S7**). Based on the predicted  
322 interactions, target genes were achieved for an additional credible variant rs10898526. The SNP  
323 rs10898526 located at a pleiotropic locus prioritized by three meta-analysis methods and obtained  
324 Müller cell/astrocyte-specific open chromatin signatures. Target gene analysis based on ABC  
325 model suggested rs10898526 could interact with *ME3* gene promoter (**Figure 3B**). We found *ME3*  
326 was documented to involve in the oxidative decarboxylation of malate to pyruvate and associated  
327 with macular thickness<sup>66</sup>. Finally, for other credible variants without evidence of active chromatin  
328 marks or chromosome interactions, we annotated the nearest gene as the target gene for the top  
329 credible variant at the pleiotropic locus. The annotated and prioritized causal variants and their  
330 genes were shown in **Table S8**.

331

### 332 **Shared biological pathways and drug repurposing opportunities**

333 To assess the pleiotropic causal genes that affect biological pathways relevant to ocular diseases  
334 and explore the potential role of candidate genes in drug repurposing, we conducted several  
335 functional investigations. GO pathway analysis was first conducted in three orthogonal ontologies  
336 to explore the biological mechanisms of causal genes on ocular comorbidity. We detected 47  
337 significant (FDR < 0.05) pathways, including the regulation of nerve development (GO:0021675,  
338 GO:0007409, and GO:0048666) (**Figure 4A, 4B, Table S9**). Multiple protein modification  
339 pathways were also enriched, such as regulation of the protein modification process  
340 (GO:0031399), protein phosphorylation (GO:0006468), and histone h3 acetylation (GO:0043966).  
341 In addition, *EFNA3*, *EFNA4*, and *SHC1* were hub genes in the PPI network of causal genes

(**Figure 4B**). We conducted gene-phenotype relationship analysis and revealed causal gene set was enriched for skin/hair/eye pigmentation (q-value = 0.0236) and eye color (q-value = 0.0008). We then linked genes to licensed drugs and found aspirin and zopiclone targeted the causal genes *ME3* and *GABRA5* separately. By searching the approved drugs and drug targets for AMD, cataract, and glaucoma in Drugbank<sup>58</sup> and DGIdb<sup>59</sup>, we identified 88 drug targets for the ocular diseases and found 12 (40%) of the 30 causal genes interacting with these drug targets. Noteworthy, *EFNA4*, a gene identified as being involved in neuronal development in previous pathway analysis, interacted with aflibercept-targeted gene *VEGFA* and pilocarpine-targeted gene *NTRK1* in the PPI network of AMD and glaucoma (**Figure 4C**, **Figure 4D**), indicating the drug repurposing opportunities for the treatment of ocular comorbidity.

352

## 353 Discussion

354 In our study, we comprehensively investigated genetic sharing and epidemiological associations  
355 for three age-related ocular disorders. We confirmed the significant relationships among AMD,  
356 cataract, and glaucoma using a large-scale prospective observational study, genetic correlation  
357 analysis, and MR, followed by pleiotropic region analysis to explore regional pleiotropy. Ten  
358 significant pleiotropic loci of AMD, cataract, and glaucoma were identified using complementary  
359 meta-analyses, four of which achieved a marginally significant threshold in replication  
360 meta-analysis. In addition, we identified Müller cells and astrocytes as disease-associated cell  
361 types by single-cell multi-omics analysis. By incorporating statistical fine-mapping, retinal eQTL  
362 colocalization, and 3D genome loop data, we systematically prioritized causal target genes for  
363 pleiotropic variants. The interrogation of network biology was also implemented to identify

364 disease genes-associated molecules and pathways for potential drug repositioning of ocular  
365 disorders.

366

367 To our knowledge, no previous study has investigated the genetic and non-genetic associations  
368 among AMD, cataract, and glaucoma. Several observational, clinical, and genetic evidence  
369 strongly suggest a shared biological basis or similar pathophysiological mechanisms among these  
370 age-related ocular disorders<sup>2-4; 16</sup>. In this study, both epidemiological evidence based on  
371 large-scale UKBB data and genetic evidence based on several largest GWASs data supported  
372 pairwise tight associations between AMD, cataract, and glaucoma at different levels. The  
373 mechanisms behind our findings will shed light on the in-depth investigation of gene-environment  
374 interactions and comorbidity mechanisms across AMD, cataract, and glaucoma, which could also  
375 initiate further ocular disease comorbidity studies and emphasize the importance of  
376 comprehensive diagnosis and disease prevention in clinical practice.

377

378 By cross-disease meta-analysis at both variant and locus levels, we successfully identified ten  
379 pleiotropic loci. Nevertheless, understanding disease-causal cell types is of great value for the  
380 investigation of the precise mechanism between these loci-influenced genes and disease  
381 pathogenesis. We identified Müller cells and astrocytes as potential casual cell types for ocular  
382 comorbidity using two algorithms. A study claimed that Müller cells play a role in  
383 regulating serine biosynthesis, a critical part of the macular defense against oxidative stress, and  
384 their dysregulation may cause macular lesions<sup>67</sup>. Furthermore, Müller cells and astrocytes have  
385 multiple functions symbiotically associated with RGCs, such as glutamate clearance, neurotrophic

386 factor release, and neurotransmitter recycling<sup>68</sup>, and the abnormality of RGCs will cause the  
387 impairment of visual acuity. Another study reported that the loss of astrocytes, together with  
388 retinal ischemia that occurs in AMD macula, could induce the death of RGCs owing to the  
389 oxidative damage<sup>69</sup>. Despite insufficient evidence in our study, a connection between macular  
390 vascular endothelium and these ocular diseases has been widely discussed<sup>44; 70-73</sup>. As a matrix cell  
391 type, fibroblasts can be activated by matricellular proteins, resulting in abnormal fibrotic processes  
392 in the extracellular matrix and subsequent elevated intraocular pressure<sup>74</sup>. In addition, fibroblasts  
393 may be recruited to neovascular lesions and differentiate into myofibroblasts, a key cell type in  
394 macular fibrosis secondary to neovascular AMD<sup>75</sup>.

395  
396 Leveraging pleiotropic genes we found, we nominated several ocular disease-related pathways  
397 like the regulation of nerve development. The optic nerve is made up of RGC axons and transmits  
398 visual signals from photoreceptor cells to the brain. Diminution of vision will occur once the  
399 transitions were hindered. Glaucoma is a neurodegenerative disorder manifesting selective,  
400 progressive, and irreversible degeneration of the optic nerve, and optic nerve regeneration in  
401 glaucoma treatment was widely studied<sup>76-78</sup>. The photoreceptor synapses across retinas of patients  
402 with AMD retract into the outer nuclear layer which evokes the subsequent outgrowth and  
403 reformation of synaptic contacts<sup>79</sup>. Besides, optic nerve edema was found weeks to months after  
404 cataract extraction<sup>80</sup>. By conducting gene-phenotype relationship analysis, pleiotropic genes were  
405 related to eye color, which suggested the relevance to these age-related ocular diseases. Darker iris  
406 color is pertinent with increased risks of cataract and intraocular pressure and mitigated risks of  
407 AMD, uveal melanoma, and pigmentary glaucoma<sup>14; 81-84</sup>.

408

409 There are a few shortcomings in these analyses. First, the relationship between AMD and  
410 glaucoma was not consistent between genetic correlation analysis and epidemiological evidence  
411 which may be due to environmental impact factors. More studies should be conducted to clarify  
412 the relationship between AMD and glaucoma. Second, the number of glaucoma cases was much  
413 larger than those for the other two diseases, and some controls may inevitably overlap in glaucoma  
414 and cataract, which may affect the power of signals and cause systemic errors and wrongly  
415 preferential shared effect in meta-analysis. Third, in the present study, we found several cell types  
416 related to these traits, however, based on limited public annotation data, tissue-level annotation  
417 profiles were leveraged rather than cell type-specific data to identify truly causal genes. Thus,  
418 genetic information regarding the eye needs to be interpreted more precisely and accurately.  
419 Fourth, our fine-mapping only yielded credible sets of variants under the assumption of one causal  
420 variant; therefore, the prioritized causal genes may be underestimated. In addition, although we  
421 found several signs connecting certain drug targets and causal pleiotropic genes, whether these  
422 drugs are beneficial or harmful to the phenotype is still unknown. Further experiments concerning  
423 drug discovery and repurposing need to be conducted in the future.

424

## 425 **Declaration of interests**

426 The authors declare no conflict of interest.

427

## 428 **Acknowledgments**

429 This study was supported by the National Natural Science Foundation of China (Grant Numbers

430 82020108007, 81830026, 32070675) and the Beijing-Tianjin-Hebei Special Project [Grant  
431 Number 19JCZDJC64300(Z), 20JCZXJC00180].

432

#### 433 **Author contributions**

434 H.Y. and M.J.L. conceived of the project. X.Y., H.Y., and Y.J. performed the analyses. H.H., X.K.,  
435 and M.L. contributed to the data collection and processing. Y.Z., J.W., and X.F. contributed to  
436 manuscript polishing and provided analysis suggestions. X.Y., M.J.L., and H.Y. wrote the  
437 manuscript. The authors read and approved the final submission.

438

#### 439 **Data and code availability**

440 The published article includes all datasets analyzed during this study.

# Reference

1. (2021). Trends in prevalence of blindness and distance and near vision impairment over 30 years: an analysis for the Global Burden of Disease Study. The Lancet Global health 9, e130-e143.
2. Vinod, K., Gedde, S.J., Feuer, W.J., Panarelli, J.F., Chang, T.C., Chen, P.P., and Parrish, R.K., 2nd. (2017). Practice Preferences for Glaucoma Surgery: A Survey of the American Glaucoma Society. Journal of glaucoma 26, 687-693.
3. Hu, C.C., Ho, J.D., Lin, H.C., and Kao, L.T. (2017). Association between open-angle glaucoma and neovascular age-related macular degeneration: a case-control study. Eye (London, England) 31, 872-877.
4. Weill, Y., Hanhart, J., Zadok, D., Smadja, D., Gelman, E., and Abulafia, A. (2021). Patient management modifications in cataract surgery candidates following incorporation of routine preoperative macular optical coherence tomography. J Cataract Refract Surg 47, 78-82.
5. Fritsche, L.G., Igl, W., Bailey, J.N., Grassmann, F., Sengupta, S., Bragg-Gresham, J.L., Burdon, K.P., Hebbring, S.J., Wen, C., Gorski, M., et al. (2016). A large genome-wide association study of age-related macular degeneration highlights contributions of rare and common variants. Nat Genet 48, 134-143.
6. Winkler, T.W., Grassmann, F., Brandl, C., Kiel, C., Gunther, F., Strunz, T., Weidner, L., Zimmermann, M.E., Korb, C.A., Poplawski, A., et al. (2020). Genome-wide association meta-analysis for early age-related macular degeneration highlights novel loci and insights for advanced disease. BMC Med Genomics 13, 120.

- 463 7. Choquet, H., Melles, R.B., Anand, D., Yin, J., Cuellar-Partida, G., Wang, W., andMe  
464 Research, T., Hoffmann, T.J., Nair, K.S., Hysi, P.G., et al. (2021). A large multiethnic  
465 GWAS meta-analysis of cataract identifies new risk loci and sex-specific effects. Nat  
466 Commun 12, 3595.
- 467 8. Khawaja, A.P., Cooke Bailey, J.N., Wareham, N.J., Scott, R.A., Simcoe, M., Igo, R.P., Jr.,  
468 Song, Y.E., Wojciechowski, R., Cheng, C.Y., Khaw, P.T., et al. (2018). Genome-wide  
469 analyses identify 68 new loci associated with intraocular pressure and improve risk  
470 prediction for primary open-angle glaucoma. Nat Genet 50, 778-782.
- 471 9. Gharahkhani, P., Jorgenson, E., Hysi, P., Khawaja, A.P., Pendergrass, S., Han, X., Ong,  
472 J.S., Hewitt, A.W., Segre, A.V., Rouhana, J.M., et al. (2021). Genome-wide  
473 meta-analysis identifies 127 open-angle glaucoma loci with consistent effect across  
474 ancestries. Nat Commun 12, 1258.
- 475 10. Mackey, D.A., and Hewitt, A.W. (2014). Genome-wide association study success in  
476 ophthalmology. Curr Opin Ophthalmol 25, 386-393.
- 477 11. Seddon, J.M., Cote, J., Page, W.F., Aggen, S.H., and Neale, M.C. (2005). The US twin  
478 study of age-related macular degeneration: relative roles of genetic and environmental  
479 influences. Arch Ophthalmol 123, 321-327.
- 480 12. Hammond, C.J., Snieder, H., Spector, T.D., and Gilbert, C.E. (2000). Genetic and  
481 environmental factors in age-related nuclear cataracts in monozygotic and dizygotic  
482 twins. N Engl J Med 342, 1786-1790.
- 483 13. Yonova-Doing, E., Forkin, Z.A., Hysi, P.G., Williams, K.M., Spector, T.D., Gilbert, C.E., and  
484 Hammond, C.J. (2016). Genetic and Dietary Factors Influencing the Progression of

485 Nuclear Cataract. *Ophthalmology* 123, 1237-1244.

486 14. Simcoe, M.J., Weisschuh, N., Wissinger, B., Hysi, P.G., and Hammond, C.J. (2020).

487 Genetic Heritability of Pigmentary Glaucoma and Associations With Other Eye

488 Phenotypes. *JAMA ophthalmology* 138, 294-299.

489 15. van Koolwijk, L.M., Despriet, D.D., van Duijn, C.M., Pardo Cortes, L.M., Vingerling, J.R.,

490 Aulchenko, Y.S., Oostra, B.A., Klaver, C.C., and Lemij, H.G. (2007). Genetic

491 contributions to glaucoma: heritability of intraocular pressure, retinal nerve fiber layer

492 thickness, and optic disc morphology. *Investigative ophthalmology & visual science* 48,

493 3669-3676.

494 16. Grassmann, F., Kiel, C., Zimmermann, M.E., Gorski, M., Grassmann, V., Stark, K.,

495 International, A.M.D.G.C., Heid, I.M., and Weber, B.H. (2017). Genetic pleiotropy

496 between age-related macular degeneration and 16 complex diseases and traits.

497 *Genome Med* 9, 29.

498 17. Cuellar-Partida, G., Craig, J.E., Burdon, K.P., Wang, J.J., Vote, B.J., Souzeau, E.,

499 McAllister, I.L., Isaacs, T., Lake, S., Mackey, D.A., et al. (2016). Assessment of

500 polygenic effects links primary open-angle glaucoma and age-related macular

501 degeneration. *Scientific reports* 6, 26885.

502 18. Xue, Z., Yuan, J., Chen, F., Yao, Y., Xing, S., Yu, X., Li, K., Wang, C., Bao, J., Qu, J., et al.

503 (2022). Genome-wide association meta-analysis of 88,250 individuals highlights

504 pleiotropic mechanisms of five ocular diseases in UK Biobank. *EBioMedicine* 82,

505 104161.

506 19. Ratnapriya, R., Sosina, O.A., Starostik, M.R., Kwicklis, M., Kapphahn, R.J., Fritsche, L.G.,

507 Walton, A., Arvanitis, M., Gieser, L., Pietraszkiewicz, A., et al. (2019). Retinal  
508 transcriptome and eQTL analyses identify genes associated with age-related macular  
509 degeneration. *Nature genetics* 51, 606-610.

510 20. Orozco, L.D., Chen, H.H., Cox, C., Katschke, K.J., Jr., Arceo, R., Espiritu, C., Caplazi, P.,  
511 Nghiem, S.S., Chen, Y.J., Modrusan, Z., et al. (2020). Integration of eQTL and a  
512 Single-Cell Atlas in the Human Eye Identifies Causal Genes for Age-Related Macular  
513 Degeneration. *Cell reports* 30, 1246-1259.e1246.

514 21. Menon, M., Mohammadi, S., Davila-Velderrain, J., Goods, B.A., Cadwell, T.D., Xing, Y.,  
515 Stemmer-Rachamimov, A., Shalek, A.K., Love, J.C., Kellis, M., et al. (2019).  
516 Single-cell transcriptomic atlas of the human retina identifies cell types associated with  
517 age-related macular degeneration. *Nat Commun* 10, 4902.

518 22. Wang, J., Zibetti, C., Shang, P., Sripathi, S.R., Zhang, P., Cano, M., Hoang, T., Xia, S., Ji,  
519 H., Merbs, S.L., et al. (2018). ATAC-Seq analysis reveals a widespread decrease of  
520 chromatin accessibility in age-related macular degeneration. *Nature communications*  
521 9, 1364.

522 23. Wang, S.K., Nair, S., Li, R., Kraft, K., Pampari, A., Patel, A., Kang, J.B., Luong, C.,  
523 Kundaje, A., and Chang, H.Y. (2022). Single-cell multiome of the human retina and  
524 deep learning nominate causal variants in complex eye diseases. *bioRxiv*,  
525 2022.2003.2009.483684.

526 24. Buniello, A., MacArthur, J.A.L., Cerezo, M., Harris, L.W., Hayhurst, J., Malangone, C.,  
527 McMahon, A., Morales, J., Mountjoy, E., Sollis, E., et al. (2019). The NHGRI-EBI  
528 GWAS Catalog of published genome-wide association studies, targeted arrays and

529 summary statistics 2019. Nucleic acids research 47, D1005-d1012.

530 25. Sudlow, C., Gallacher, J., Allen, N., Beral, V., Burton, P., Danesh, J., Downey, P., Elliott, P.,

531 Green, J., Landray, M., et al. (2015). UK biobank: an open access resource for

532 identifying the causes of a wide range of complex diseases of middle and old age.

533 PLoS medicine 12, e1001779.

534 26. Canela-Xandri, O., Rawlik, K., and Tenesa, A. (2018). An atlas of genetic associations in

535 UK Biobank. Nature genetics 50, 1593-1599.

536 27. Watanabe, K., Stringer, S., Frei, O., Umićević Mirkov, M., de Leeuw, C., Polderman, T.J.C.,

537 van der Sluis, S., Andreassen, O.A., Neale, B.M., and Posthuma, D. (2019). A global

538 overview of pleiotropy and genetic architecture in complex traits. Nature genetics 51,

539 1339-1348.

540 28. Zheng, J., Erzurumluoglu, A.M., Elsworth, B.L., Kemp, J.P., Howe, L., Haycock, P.C.,

541 Hemani, G., Tansey, K., Laurin, C., Pourcain, B.S., et al. (2017). LD Hub: a centralized

542 database and web interface to perform LD score regression that maximizes the

543 potential of summary level GWAS data for SNP heritability and genetic correlation

544 analysis. Bioinformatics (Oxford, England) 33, 272-279.

545 29. Leslie, R., O'Donnell, C.J., and Johnson, A.D. (2014). GRASP: analysis of

546 genotype-phenotype results from 1390 genome-wide association studies and

547 corresponding open access database. Bioinformatics (Oxford, England) 30, i185-194.

548 30. Kamat, M.A., Blackshaw, J.A., Young, R., Surendran, P., Burgess, S., Danesh, J.,

549 Butterworth, A.S., and Staley, J.R. (2019). PhenoScanner V2: an expanded tool for

550 searching human genotype-phenotype associations. Bioinformatics (Oxford, England)

551 35, 4851-4853.

552 31. Mailman, M.D., Feolo, M., Jin, Y., Kimura, M., Tryka, K., Bagoutdinov, R., Hao, L., Kiang,  
553 A., Paschall, J., Phan, L., et al. (2007). The NCBI dbGaP database of genotypes and  
554 phenotypes. *Nature genetics* 39, 1181-1186.

555 32. Kurki, M.I., Karjalainen, J., Palta, P., Sipilä, T.P., Kristiansson, K., Donner, K., Reeve, M.P.,  
556 Laivuori, H., Aavikko, M., Kaunisto, M.A., et al. (2022). FinnGen: Unique genetic  
557 insights from combining isolated population and national health register data. *medRxiv*,  
558 2022.2003.2003.22271360.

559 33. Bulik-Sullivan, B., Finucane, H.K., Anttila, V., Gusev, A., Day, F.R., Loh, P.R., Duncan, L.,  
560 Perry, J.R., Patterson, N., Robinson, E.B., et al. (2015). An atlas of genetic  
561 correlations across human diseases and traits. *Nature genetics* 47, 1236-1241.

562 34. Zhang, Q., Privé, F., Vilhjálmsson, B., and Speed, D. (2021). Improved genetic prediction  
563 of complex traits from individual-level data or summary statistics. *Nature*  
564 *communications* 12, 4192.

565 35. Hemani, G., Zheng, J., Elsworth, B., Wade, K.H., Haberland, V., Baird, D., Laurin, C.,  
566 Burgess, S., Bowden, J., Langdon, R., et al. (2018). The MR-Base platform supports  
567 systematic causal inference across the human phenome. *eLife* 7.

568 36. Sherry, S.T., Ward, M.H., Kholodov, M., Baker, J., Phan, L., Smigielski, E.M., and Sirotkin,  
569 K. (2001). dbSNP: the NCBI database of genetic variation. *Nucleic acids research* 29,  
570 308-311.

571 37. Pickrell, J.K., Berisa, T., Liu, J.Z., Séguérel, L., Tung, J.Y., and Hinds, D.A. (2016).  
572 Detection and interpretation of shared genetic influences on 42 human traits. *Nature*

573 genetics 48, 709-717.

574 38. Bhattacharjee, S., Rajaraman, P., Jacobs, K.B., Wheeler, W.A., Melin, B.S., Hartge, P.,

575 Yeager, M., Chung, C.C., Chanock, S.J., and Chatterjee, N. (2012). A subset-based

576 approach improves power and interpretation for the combined analysis of genetic

577 association studies of heterogeneous traits. *American journal of human genetics* 90,

578 821-835.

579 39. Willer, C.J., Li, Y., and Abecasis, G.R. (2010). METAL: fast and efficient meta-analysis of

580 genomewide association scans. *Bioinformatics (Oxford, England)* 26, 2190-2191.

581 40. Andreassen, O.A., Thompson, W.K., Schork, A.J., Ripke, S., Mattingsdal, M., Kelsoe, J.R.,

582 Kendler, K.S., O'Donovan, M.C., Rujescu, D., Werge, T., et al. (2013). Improved

583 detection of common variants associated with schizophrenia and bipolar disorder

584 using pleiotropy-informed conditional false discovery rate. *PLoS genetics* 9,

585 e1003455.

586 41. Purcell, S., Neale, B., Todd-Brown, K., Thomas, L., Ferreira, M.A., Bender, D., Maller, J.,

587 Sklar, P., de Bakker, P.I., Daly, M.J., et al. (2007). PLINK: a tool set for whole-genome

588 association and population-based linkage analyses. *American journal of human*

589 *genetics* 81, 559-575.

590 42. Auton, A., Brooks, L.D., Durbin, R.M., Garrison, E.P., Kang, H.M., Korbel, J.O., Marchini,

591 J.L., McCarthy, S., McVean, G.A., and Abecasis, G.R. (2015). A global reference for

592 human genetic variation. *Nature* 526, 68-74.

593 43. de Leeuw, C.A., Mooij, J.M., Heskes, T., and Posthuma, D. (2015). MAGMA: generalized

594 gene-set analysis of GWAS data. *PLoS computational biology* 11, e1004219.

595 44. Voigt, A.P., Mulfaul, K., Mullin, N.K., Flamme-Wiese, M.J., Giacalone, J.C., Stone, E.M.,  
596 Tucker, B.A., Scheetz, T.E., and Mullins, R.F. (2019). Single-cell transcriptomics of  
597 the human retinal pigment epithelium and choroid in health and macular degeneration.  
598 Proceedings of the National Academy of Sciences of the United States of America 116,  
599 24100-24107.

600 45. van Zyl, T., Yan, W., McAdams, A., Peng, Y.R., Shekhar, K., Regev, A., Juric, D., and  
601 Sanes, J.R. (2020). Cell atlas of aqueous humor outflow pathways in eyes of humans  
602 and four model species provides insight into glaucoma pathogenesis. Proceedings of  
603 the National Academy of Sciences of the United States of America 117, 10339-10349.

604 46. Patel, G., Fury, W., Yang, H., Gomez-Caraballo, M., Bai, Y., Yang, T., Adler, C., Wei, Y., Ni,  
605 M., Schmitt, H., et al. (2020). Molecular taxonomy of human ocular outflow tissues  
606 defined by single-cell transcriptomics. Proceedings of the National Academy of  
607 Sciences of the United States of America 117, 12856-12867.

608 47. Zheng, G.X., Terry, J.M., Belgrader, P., Ryvkin, P., Bent, Z.W., Wilson, R., Ziraldo, S.B.,  
609 Wheeler, T.D., McDermott, G.P., Zhu, J., et al. (2017). Massively parallel digital  
610 transcriptional profiling of single cells. Nature communications 8, 14049.

611 48. Hao, Y., Hao, S., Andersen-Nissen, E., Mauck, W.M., 3rd, Zheng, S., Butler, A., Lee, M.J.,  
612 Wilk, A.J., Darby, C., Zager, M., et al. (2021). Integrated analysis of multimodal  
613 single-cell data. Cell 184, 3573-3587.e3529.

614 49. Durinck, S., Spellman, P.T., Birney, E., and Huber, W. (2009). Mapping identifiers for the  
615 integration of genomic datasets with the R/Bioconductor package biomaRt. Nature  
616 protocols 4, 1184-1191.

617 50. Strunz, T., Kiel, C., Grassmann, F., Ratnapriya, R., Kwicklis, M., Karlstetter, M., Fauser, S.,  
618 Arend, N., Swaroop, A., Langmann, T., et al. (2020). A mega-analysis of expression  
619 quantitative trait loci in retinal tissue. *PLoS genetics* 16, e1008934.

620 51. Giambartolomei, C., Vukcevic, D., Schadt, E.E., Franke, L., Hingorani, A.D., Wallace, C.,  
621 and Plagnol, V. (2014). Bayesian test for colocalisation between pairs of genetic  
622 association studies using summary statistics. *PLoS genetics* 10, e1004383.

623 52. Cherry, T.J., Yang, M.G., Harmin, D.A., Tao, P., Timms, A.E., Bauwens, M., Allikmets, R.,  
624 Jones, E.M., Chen, R., De Baere, E., et al. (2020). Mapping the cis-regulatory  
625 architecture of the human retina reveals noncoding genetic variation in disease.  
626 *Proceedings of the National Academy of Sciences of the United States of America* 117,  
627 9001-9012.

628 53. Fulco, C.P., Nasser, J., Jones, T.R., Munson, G., Bergman, D.T., Subramanian, V.,  
629 Grossman, S.R., Anyoha, R., Doughty, B.R., Patwardhan, T.A., et al. (2019).  
630 Activity-by-contact model of enhancer-promoter regulation from thousands of CRISPR  
631 perturbations. *Nature genetics* 51, 1664-1669.

632 54. Weissbrod, O., Hormozdiari, F., Benner, C., Cui, R., Ulirsch, J., Gazal, S., Schoech, A.P.,  
633 van de Geijn, B., Reshef, Y., Márquez-Luna, C., et al. (2020). Functionally informed  
634 fine-mapping and polygenic localization of complex trait heritability. *Nature genetics*  
635 52, 1355-1363.

636 55. Wang, G., Sarkar, A., Carbonetto, P., and Stephens, M. (2020). A simple new approach to  
637 variable selection in regression, with application to genetic fine mapping. *Journal of*  
638 *the Royal Statistical Society: Series B (Statistical Methodology)* 82, 1273-1300.

639 56. Szklarczyk, D., Gable, A.L., Lyon, D., Junge, A., Wyder, S., Huerta-Cepas, J., Simonovic,  
640 M., Doncheva, N.T., Morris, J.H., Bork, P., et al. (2019). STRING v11: protein-protein  
641 association networks with increased coverage, supporting functional discovery in  
642 genome-wide experimental datasets. *Nucleic acids research* 47, D607-d613.

643 57. Xie, Z., Bailey, A., Kuleshov, M.V., Clarke, D.J.B., Evangelista, J.E., Jenkins, S.L.,  
644 Lachmann, A., Wojciechowicz, M.L., Kropiwnicki, E., Jagodnik, K.M., et al. (2021).  
645 Gene Set Knowledge Discovery with Enrichr. *Current protocols* 1, e90.

646 58. Wishart, D.S., Knox, C., Guo, A.C., Shrivastava, S., Hassanali, M., Stothard, P., Chang, Z.,  
647 and Woolsey, J. (2006). DrugBank: a comprehensive resource for in silico drug  
648 discovery and exploration. *Nucleic acids research* 34, D668-672.

649 59. Freshour, S.L., Kiwala, S., Cotto, K.C., Coffman, A.C., McMichael, J.F., Song, J.J., Griffith,  
650 M., Griffith, O.L., and Wagner, A.H. (2021). Integration of the Drug-Gene Interaction  
651 Database (DGIdb 4.0) with open crowdsourcing efforts. *Nucleic acids research* 49,  
652 D1144-d1151.

653 60. Shannon, P., Markiel, A., Ozier, O., Baliga, N.S., Wang, J.T., Ramage, D., Amin, N.,  
654 Schwikowski, B., and Ideker, T. (2003). Cytoscape: a software environment for  
655 integrated models of biomolecular interaction networks. *Genome research* 13,  
656 2498-2504.

657 61. Zhang, J., Qiu, Q., Wang, H., Chen, C., and Luo, D. (2021). TRIM46 contributes to high  
658 glucose-induced ferroptosis and cell growth inhibition in human retinal capillary  
659 endothelial cells by facilitating GPX4 ubiquitination. *Experimental cell research* 407,  
660 112800.

661 62. Goldshmit, Y., Galea, M.P., Wise, G., Bartlett, P.F., and Turnley, A.M. (2004). Axonal  
662 regeneration and lack of astrocytic gliosis in EphA4-deficient mice. The Journal of  
663 neuroscience : the official journal of the Society for Neuroscience 24, 10064-10073.

664 63. Kozulin, P., Natoli, R., O'Brien, K.M., Madigan, M.C., and Provis, J.M. (2009). Differential  
665 expression of anti-angiogenic factors and guidance genes in the developing macula.  
666 Molecular vision 15, 45-59.

667 64. Zeng, Z., Gao, Z.L., Zhang, Z.P., Jiang, H.B., Yang, C.Q., Yang, J., and Xia, X.B. (2019).  
668 Downregulation of CKS1B restrains the proliferation, migration, invasion and  
669 angiogenesis of retinoblastoma cells through the MEK/ERK signaling pathway.  
670 International journal of molecular medicine 44, 103-114.

671 65. Zhou, H., Su, J., Hu, X., Zhou, C., Li, H., Chen, Z., Xiao, Q., Wang, B., Wu, W., Sun, Y., et  
672 al. (2020). Glia-to-Neuron Conversion by CRISPR-CasRx Alleviates Symptoms of  
673 Neurological Disease in Mice. Cell 181, 590-603.e516.

674 66. Francis, P.J. (2011). The influence of genetics on response to treatment with ranibizumab  
675 (Lucentis) for age-related macular degeneration: the Lucentis Genotype Study (an  
676 American Ophthalmological Society thesis). Transactions of the American  
677 Ophthalmological Society 109, 115-156.

678 67. Zhang, T., Zhu, L., Madigan, M.C., Liu, W., Shen, W., Cherepanoff, S., Zhou, F., Zeng, S.,  
679 Du, J., and Gillies, M.C. (2019). Human macular Müller cells rely more on serine  
680 biosynthesis to combat oxidative stress than those from the periphery. eLife 8.

681 68. García-Bermúdez, M.Y., Freude, K.K., Mouhammad, Z.A., van Wijngaarden, P., Martin,  
682 K.K., and Kolko, M. (2021). Glial Cells in Glaucoma: Friends, Foes, and Potential

683           Therapeutic Targets. *Frontiers in neurology* 12, 624983.

684   69. Ramírez, J.M., Ramírez, A.I., Salazar, J.J., de Hoz, R., and Triviño, A. (2001). Changes of

685           astrocytes in retinal ageing and age-related macular degeneration. *Experimental eye*

686           research 73, 601-615.

687   70. Fu, D.J., Keenan, T.D., Faes, L., Lim, E., Wagner, S.K., Moraes, G., Huemer, J., Kern, C.,

688           Patel, P.J., Balaskas, K., et al. (2021). Insights From Survival Analyses During 12

689           Years of Anti-Vascular Endothelial Growth Factor Therapy for Neovascular

690           Age-Related Macular Degeneration. *JAMA ophthalmology* 139, 57-67.

691   71. Klein, B.E., Klein, R., Lee, K.E., Knudtson, M.D., and Tsai, M.Y. (2006). Markers of

692           inflammation, vascular endothelial dysfunction, and age-related cataract. *American*

693           journal of ophthalmology 141, 116-122.

694   72. Bukhari, S.M., Kiu, K.Y., Thambiraja, R., Sulong, S., Rasool, A.H., and Liza-Sharmini, A.T.

695           (2016). Microvascular endothelial function and severity of primary open angle

696           glaucoma. *Eye (London, England)* 30, 1579-1587.

697   73. Su, W.W., Cheng, S.T., Ho, W.J., Tsay, P.K., Wu, S.C., and Chang, S.H. (2008).

698           Glaucoma is associated with peripheral vascular endothelial dysfunction.

699           *Ophthalmology* 115, 1173-1178.e1171.

700   74. Wallace, D.M., Murphy-Ullrich, J.E., Downs, J.C., and O'Brien, C.J. (2014). The role of

701           matricellular proteins in glaucoma. *Matrix biology : journal of the International Society*

702           for Matrix Biology 37, 174-182.

703   75. Little, K., Ma, J.H., Yang, N., Chen, M., and Xu, H. (2018). Myofibroblasts in macular

704           fibrosis secondary to neovascular age-related macular degeneration - the potential

705 sources and molecular cues for their recruitment and activation. EBioMedicine 38,  
706 283-291.

707 76. Yuan, F., Wang, M., Jin, K., and Xiang, M. (2021). Advances in Regeneration of Retinal  
708 Ganglion Cells and Optic Nerves. International journal of molecular sciences 22.

709 77. You, M., Rong, R., Zeng, Z., Xia, X., and Ji, D. (2021). Transneuronal Degeneration in the  
710 Brain During Glaucoma. Frontiers in aging neuroscience 13, 643685.

711 78. Williams, P.R., Benowitz, L.I., Goldberg, J.L., and He, Z. (2020). Axon Regeneration in the  
712 Mammalian Optic Nerve. Annual review of vision science 6, 195-213.

713 79. Sullivan, R.K., Woldemussie, E., and Pow, D.V. (2007). Dendritic and synaptic plasticity of  
714 neurons in the human age-related macular degeneration retina. Investigative  
715 ophthalmology & visual science 48, 2782-2791.

716 80. McCulley, T.J. (2012). Ischemic optic neuropathy and cataract extraction: What do I need  
717 to know? Oman journal of ophthalmology 5, 141-143.

718 81. Sun, H.P., Lin, Y., and Pan, C.W. (2014). Iris color and associated pathological ocular  
719 complications: a review of epidemiologic studies. International journal of  
720 ophthalmology 7, 872-878.

721 82. Mitchell, R., Rochtchina, E., Lee, A., Wang, J.J., and Mitchell, P. (2003). Iris color and  
722 intraocular pressure: the Blue Mountains Eye Study. American journal of  
723 ophthalmology 135, 384-386.

724 83. McGowan, A., Silvestri, G., Moore, E., Silvestri, V., Patterson, C.C., Maxwell, A.P., and  
725 McKay, G.J. (2014). Retinal vascular caliber, iris color, and age-related macular  
726 degeneration in the Irish Nun Eye Study. Investigative ophthalmology & visual science

727                    56, 382-387.

728       84. Frank, R.N., Puklin, J.E., Stock, C., and Canter, L.A. (2000). Race, iris color, and

729                    age-related macular degeneration. Transactions of the American Ophthalmological

730                    Society 98, 109-115; discussion 115-107.

731

732

## 733 **Figure legends**

### 734 **Figure 1. Genetic pleiotropy of ocular disorders at the genomic level and regional level.**

735 **A.** Epidemiological and genetic correlations between AMD, cataract, and glaucoma. Significant  
736 and strongest genetic correlations of disparate methods are shown. Red: hazard ratios estimated by  
737 Cox regression; blue: genetic correlations estimated by LDSC; yellow: genetic correlations  
738 estimated by LDAK. **B.** Genetic correlations of AMD, cataract, and glaucoma estimated by LDSC.  
739 The size and color of circles show the genetic correlations of disease pairs and the black stars  
740 indicate significant results and. **C.** Multi-state models for the role of glaucoma in transitions to  
741 other two diseases. **D.** Multi-state models for the role of cataract in transitions to other two  
742 diseases. **E.** Multi-state models for the role of AMD in transitions to other two diseases. **D.**  
743 Chromosome graphics showing the pleiotropic regions assessed by gwas-pw. A partial enlarged  
744 view shows the pleiotropic region resided in chromosome 9 which overlapped with one locus  
745 identified by meta-analysis. Different color dots represent the posterior probability of trait pairs  
746 (red: AMD-cataract; blue: AMD-glaucoma; green: cataract-glaucoma). The dashed line represents  
747 the predictive threshold of posterior probability  $> 0.6$ .

### 748 **Figure 2. The pleiotropic loci of ocular phenotypes as well as trait-associated cell types.**

749 **A.** Circular Manhattan plot of the meta-analysis results using one-sided ASSET. The orange  
750 triangles denote the lead SNPs of pleiotropic loci identified by three meta-analysis methods. The  
751 texts beside triangles show the nearest genes of these loci. The arcs in the outer layer represent  
752 chromosome positions and the number of SNPs in each position is depicted with different colors.  
753 Each dot in the inner layer represents a SNP and the red circle indicates the genome-wide  
754 significant threshold ( $P\text{-value} = 5 \times 10^{-8}$ ). **B.** The significance of various cell types from

MAGMA and LDSC in the cell-type trait association analysis. The significant cell types after Benjamini-Hochberg correction ( $FDR < 0.05$ ) are highlighted. **C.** Locus-compare plots of lead SNP rs3766916 with macular eQTL gene TRIM46. Different colors of dots represent the linkage disequilibrium between the lead SNP (colored purple) and corresponding SNP. **D.** Locuszoom plots of one-sided ASSET associations and posterior probability of causality for variants around risk SNP rs4845712 which overlaps with *EFNA3* enhancer and retinal H3K27ac HiChIP data. The risk variant is uniquely highlighted with purple and all other SNPs are highlighted by their  $r^2$ . The overlapped open chromatin peaks of 13 retinal cell types are shown in the middle. Anchor regions of the retina are highlighted with an orange or blue rectangle and red arcs show the enhance-gene pairs predicted by Activity-by-Contact model. Genes in red and blue represent the sense and antisense directions, respectively. The dashed line indicated the interested SNP position.

**Figure 3. Integration with retinal eQTLs, epigenomic, and 3D genome data for causal genes prioritization.**

**A.** Locuszoom plots of one-sided ASSET associations and posterior probability of causality for variants around risk SNP rs351973 which reside in one of the HiChIP anchors. **B.** Locuszoom plots of one-sided ASSET associations and posterior probability of causality for variants around risk SNP rs10898526 which overlaps with *ME3* predicted enhancer. The risk variant is uniquely highlighted with purple and all other SNPs are highlighted by their  $r^2$ . The overlapped open chromatin peaks of 13 retinal cell types were shown in the middle. Anchor regions of the retina were highlighted with an orange or blue rectangle and red arcs show the enhance-gene pairs predicted by Activity-by-Contact model. Genes in red and blue represent the sense and antisense directions, respectively. The dashed line indicated the interested SNP position.

777 **Figure 4. Functional enrichment of pleiotropic causal genes and drug repositioning for the**  
778 **treatment of ocular comorbidity.**

779 **A.** Gene ontology pathway enrichment analysis of pleiotropic causal genes. The size and color of  
780 the circles indicated the number of causal genes and the significance in the corresponding pathway.  
781 **B.** Protein-protein interaction (PPI) network of causal genes. The red text with larger nodes  
782 indicated the pleiotropic gene in three diseases while the purple text indicated pleiotropic genes in  
783 two diseases. The thickness of the edges represents the strength of evidence. **C. & D.** PPI  
784 networks using disease-risk genes (red) and drug-targeted genes (purple and light gray). The nodes  
785 in light blue ellipses represent the lateral drug target genes.

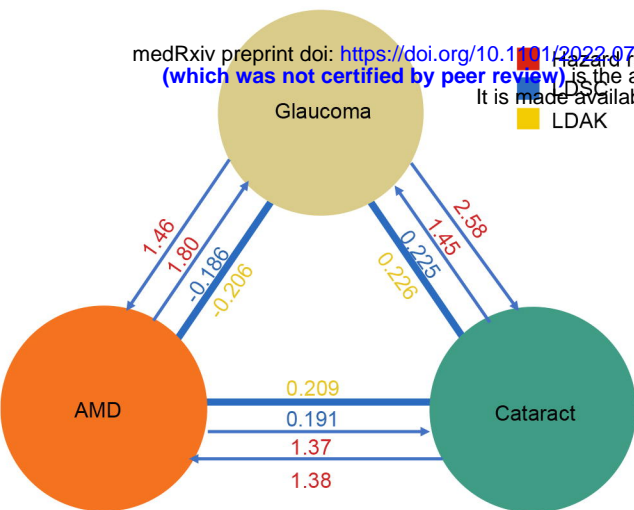
## Tables

**Table 1. The ten pleiotropic loci identified by three meta-analysis approaches**

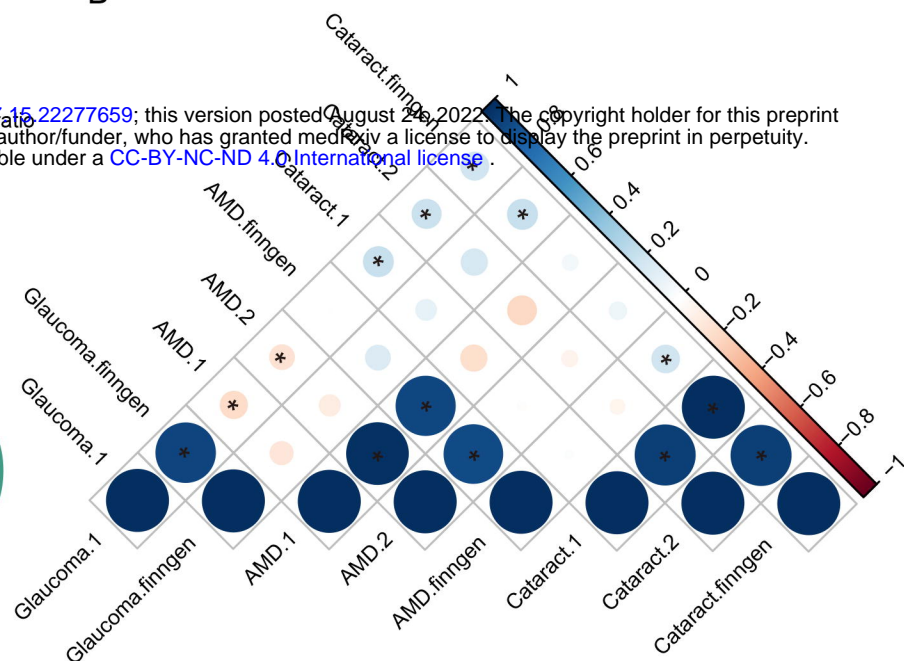
Chr	SNP ID	Position	P-value	A1	A2	Diseases	Nearest gene(s)
1	rs3766916	155049402	3.03E-09	T	C	glaucoma, AMD, cataract	<i>EFNA3</i>
3	rs35050931	150058352	6.69E-11	T	A	glaucoma, cataract	<i>TSC22D2</i>
5	rs17421627	87847586	1.83E-08	T	G	glaucoma, AMD	<i>LINC00461</i>
6	rs13191376	45522139	1.66E-09	C	T	glaucoma, cataract	<i>RUNX2</i>
7	rs12670840	116125172	7.52E-21	C	T	glaucoma, AMD, cataract	<i>CAV2</i>
9	rs944801	22051670	8.00E-42	G	C	glaucoma, cataract	<i>CDKN2B-AS1</i>
11	rs1619882	86363742	2.73E-17	C	A	glaucoma, AMD, cataract	<i>ME3</i>
11	rs11018564	89035134	2.89E-08	T	C	glaucoma, cataract	<i>TYR, NOX4</i>
15	rs1129038	28356859	5.26E-13	C	T	glaucoma, AMD, cataract	<i>HERC2</i>
19	rs146447071	818751	5.40E-09	T	C	glaucoma, cataract	<i>LPPR3</i>

A

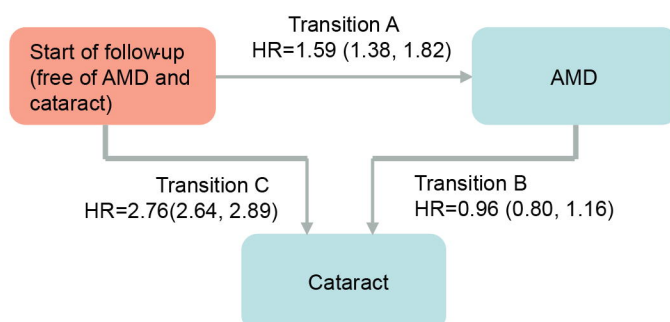
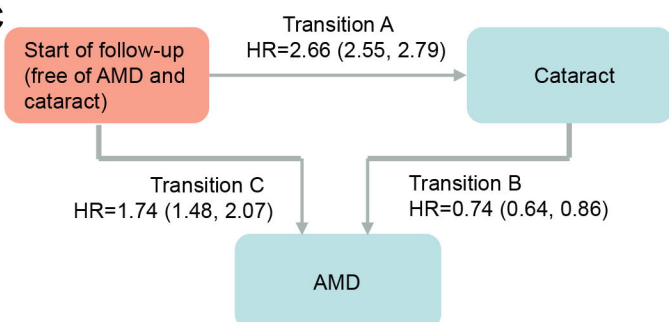
medRxiv preprint doi: <https://doi.org/10.1101/2022.07.15.22277659>; this version posted August 29, 2022. The copyright holder for this preprint (which was not certified by peer review) is the author/funder, who has granted medRxiv a license to display the preprint in perpetuity. It is made available under a CC-BY-NC-ND 4.0 International license.



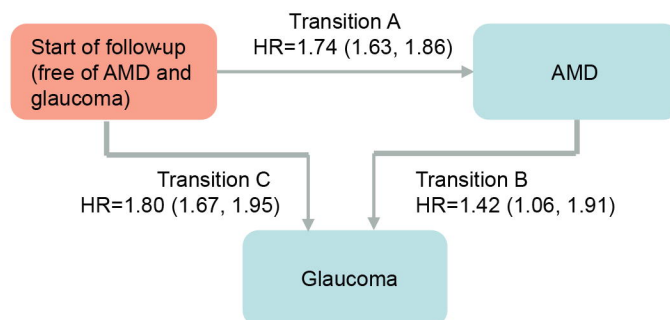
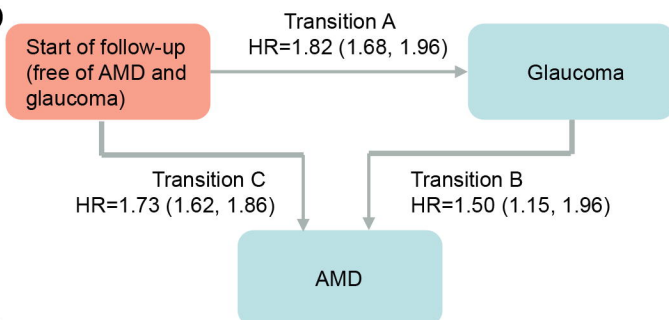
B



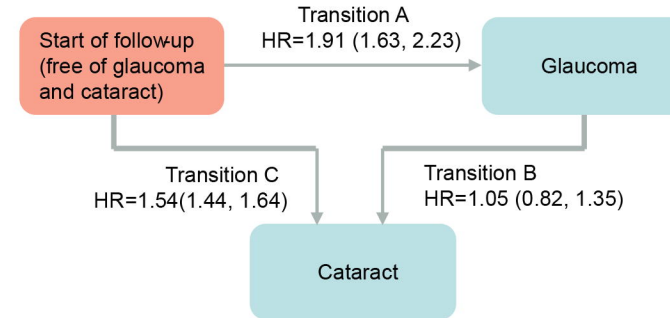
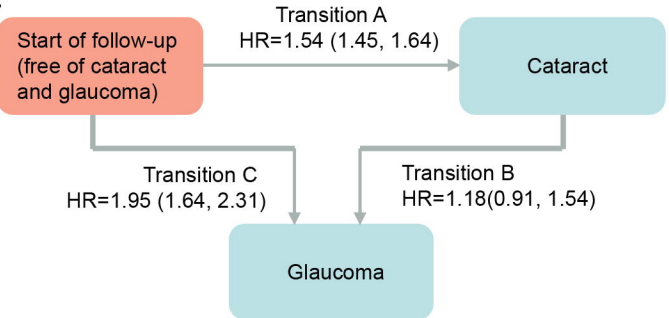
C



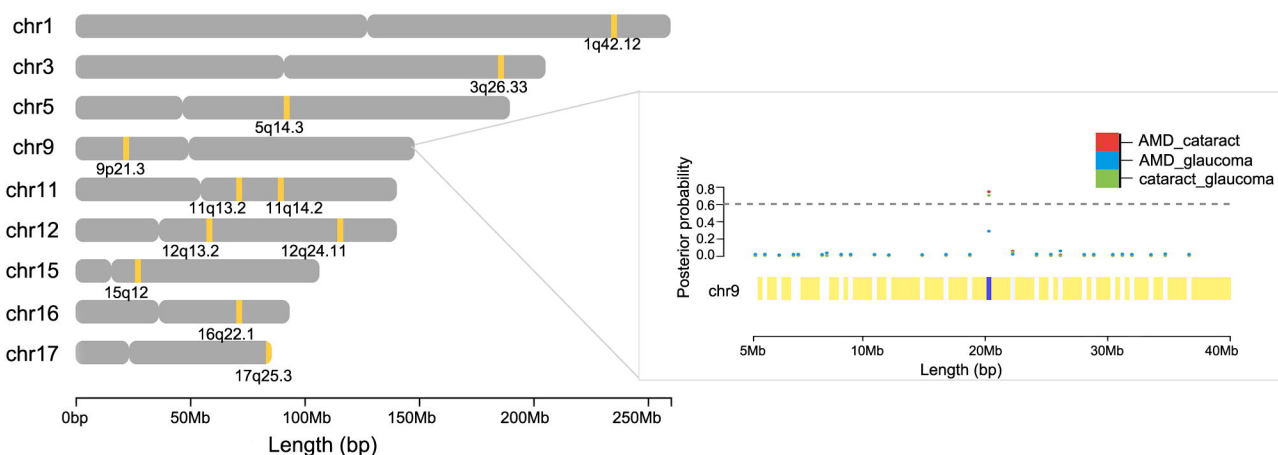
D



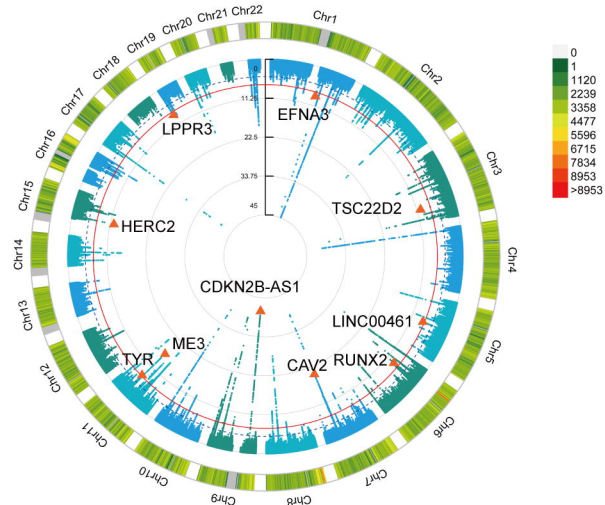
E



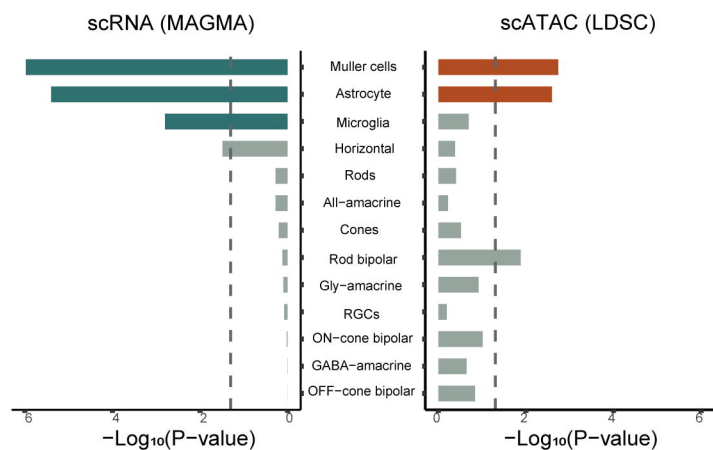
F



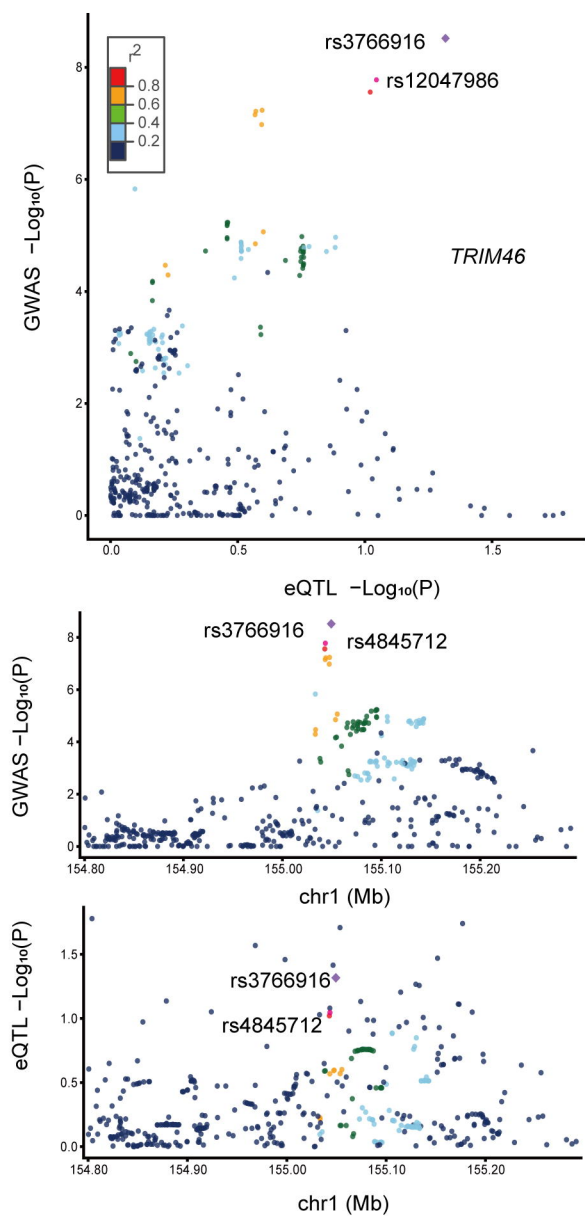
A



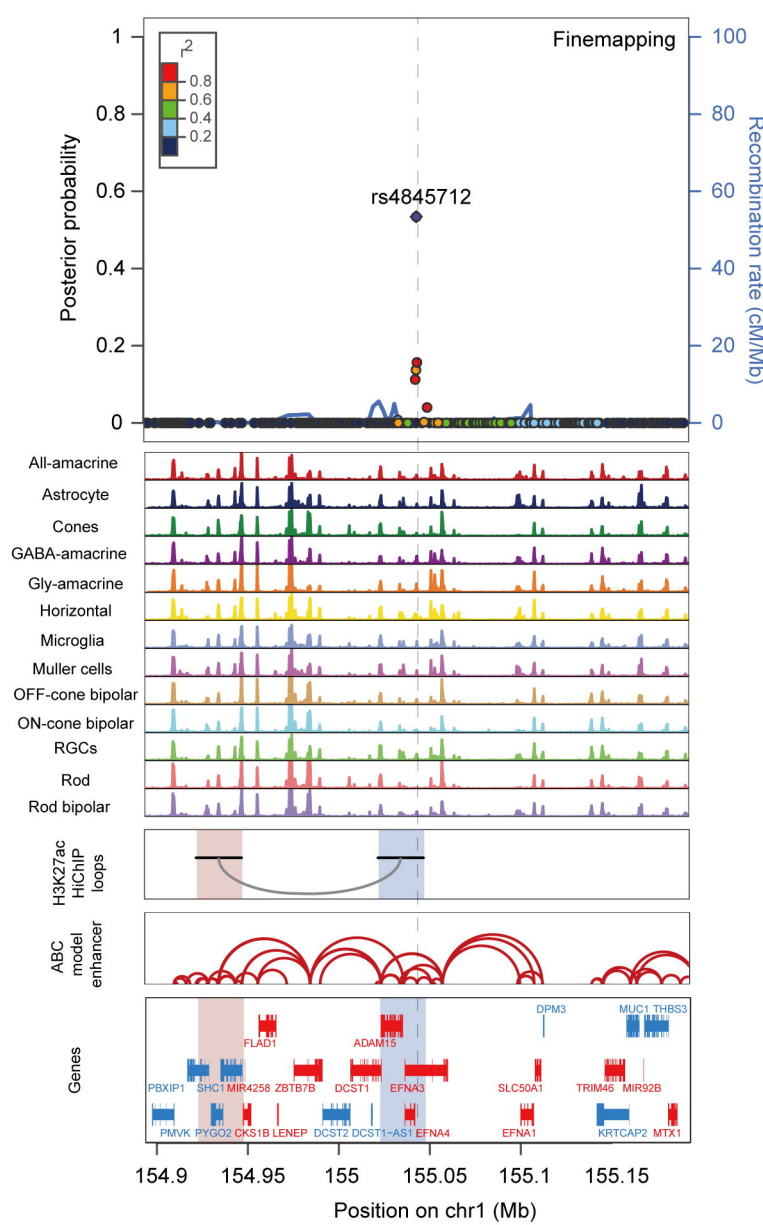
B



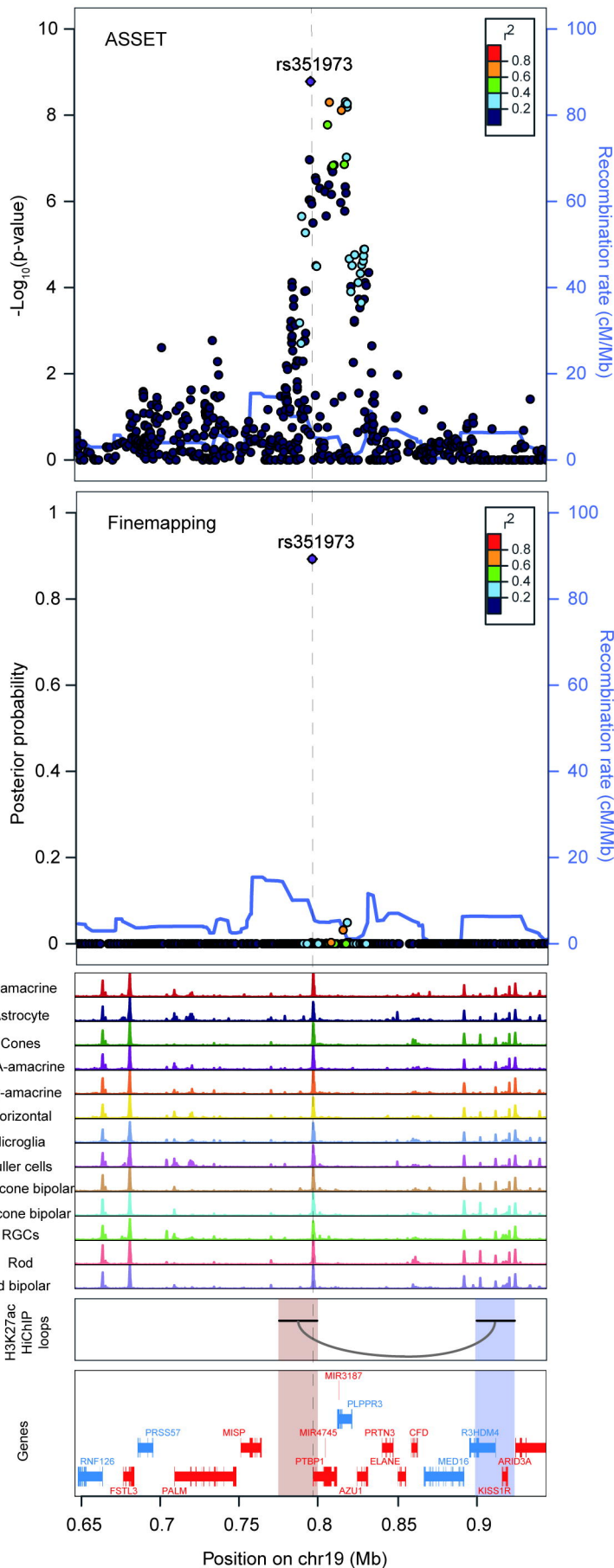
C



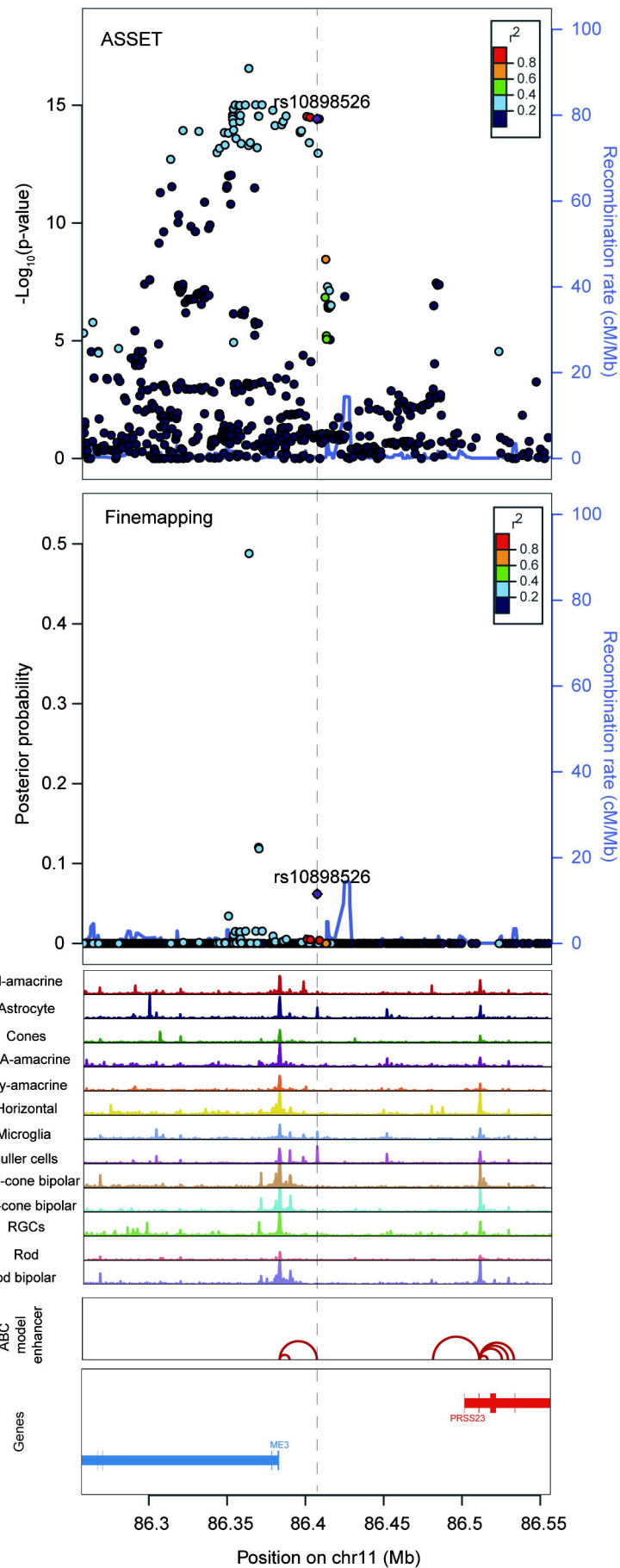
D



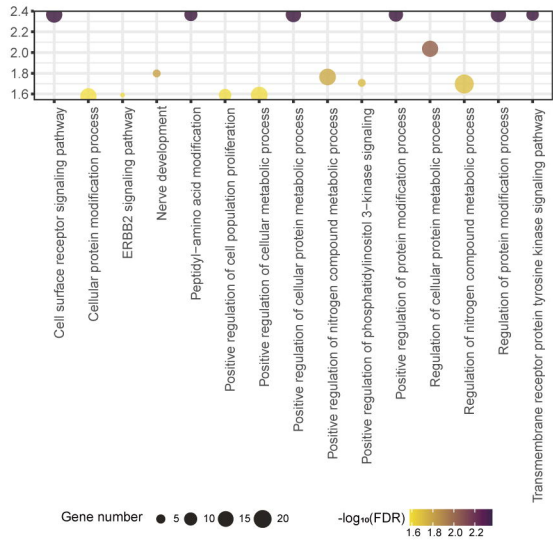
A



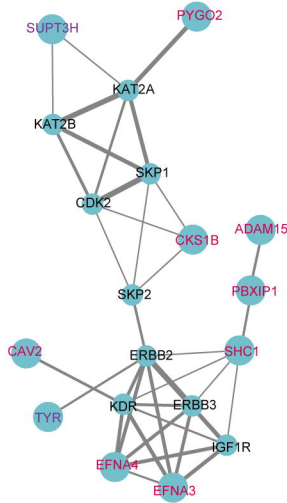
B



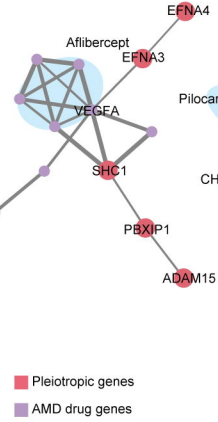
A



B



C



D

